Available online at www.sciencedirect.com
SCIENCE DIRECT
ELSEVIER
Journal of the European Ceramic Society 26 (2006) 831–836
ECERS
www.elsevier.com/locate/jeurceramsoc

Properties and vibrational spectra of magnesium phosphate glasses for nuclear waste immobilization

Toshinori Okura *, Tomoko Miyachi, Hideki Monma

Department of Materials Science and Technology, Faculty of Engineering, Kogakuin University, 2665-1, Nakano, Hachioji, Tokyo 192-0015, Japan

Available online 8 August 2005

Abstract

The leaching behavior and structure of magnesium phosphate glasses containing 45–55 mol% MgO incorporated with simulated high level nuclear wastes (HLW) were studied. The leach rate of the waste glasses decrease with increasing of the simulated HLW content. The gross leach rate of the glass waste form containing 50 mol% MgO and 45 mass% simulated HLW is of the order of 10^{-6} g/cm^2 day at 90 °C, which is small enough as compared with the corresponding release from a currently used borosilicate glass waste form. The isolated ions such as dimeric $(P_2O_7)^{4-}$ and monomeric $(PO_4)^{3-}$ ions increase upon as increasing the incorporating amount of the simulated HLW. The changes in properties can be attributed to the structure changes owing to the incorporation of the simulated HLW.

Keywords: Thermal properties; Vibrational spectra

1. Introduction

The disposal of radioactive waste generated by the nuclear fuel cycle is among the most pressing and potentially costly environmental problems. The high level nuclear wastes (HLW) are immobilized in a stable solid state and completely isolated from the biosphere.

Nuclear waste glasses are typically borosilicate glasses, and these glass compositions can experience phase separation at elevated concentrations of P_2O_5. The maximum P_2O_5 concentrations must be limited to between 1 and 3 mass%. For some waste streams, this can require considerable dilution and a substantial increase in the volume of the waste glass produced. Hence, there has been a continuing interest in developing phosphate glasses as waste forms. Furthermore, typical borosilicate glasses are limited to no more than 5 mass% actinides (2 mass% for plutonium). In contrast, iron phosphate glass with up to 15 mass% P_2O_5 can accommodate up to 40 mass% of simulated HLW.[1,2]

Phosphate glasses have some advantages over borosilicate glasses, such as a lower melting temperature and higher solubility for problematic elements, such as sulfur, and were investigated as early as the 1960s. Later work on sodium–aluminum phosphate glass[3] and iron–aluminum phosphate glass[4] showed that some of these glasses have comparable or better chemical durability than the borosilicate glasses. Present efforts are focused on the development of lead–iron phosphate glasses.[1,5–10] The main disadvantage of phosphate glass is that the melts are highly corrosive. Still, a number of the engineering problems were overcome and in the 1980s at Mayak in the Urals, considerable amounts of waste, approximately 1000 m^3, were immobilized in a phosphate glass.[11] Vitrification of wastes with Na–Al phosphate glass matrix continues today at the Mayak Production Association in Chelyabinsk where 300 million Curies of activity of HLW have been immobilized in glass. There have been studies to investigate the immobilization of Cs,[12] CsCl and SrF_2,[13] mixed-waste sludge[14] and spent nuclear fuel[2] in iron phosphate glass compositions.

Magnesium phosphate glasses are classified as ‘anomalous phosphate glasses’, which exhibit anomalies in the relationship between physical properties, such as density and

* Corresponding author. Tel.: +81 426 28 4149; fax: +81 426 28 4149.
E-mail address: okura@cc.kogakuin.ac.jp (T. Okura).

0955-2219/$ – see front matter © 2005 Elsevier Ltd. All rights reserved.
doi:10.1016/j.jeurceramsoc.2005.07.031

refractive index, and MgO/P_2O_5 (M/P) molar ratio around the metaphosphate composition (M/P = 1). The structures of M–P glasses have been studied.[15] Most of the phosphate glasses form high polyphosphate consisting of chains of phosphate ions, while the structures of M–P glasses are of two types, one includes four membered rings of PO_4 tetrahedra at M/P < 1 (type T) and the other contains dimers of PO_4 tetrahedra at M/P > 1 (type P).

In this study, M–P glasses are chosen as the base glass.[16] Simulated HLW (radioactive isotopes were not employed)[17] was incorporated into the base glass to study its effects on the properties of the glasses. The present article reports on the leach rates to water and some thermal properties. The variations of the glass structure due to the incorporation of the simulated HLW are also examined by Fourier-transformed infrared (FT-IR) and Raman spectra.

2. Experimental procedure

2.1. Sample preparation

The M–P glass frit that is used to produce glass waste form can be prepared by combining appropriate amounts of magnesium oxide and phosphoric acid and by heating at 1250 °C for 1 h. The powder mixtures of the glasses containing 0, 25 and 45 mass% of simulated HLW were melted at 1250 °C for 2 h. The melt waste glass was poured into a stainless plate. The composition of the simulated HLW is shown in Table 1.

2.2. Leach test

According to the technique of MCC-2,[18] the leach test for the glass waste forms was conducted in distilled water. About 1 g of each sample crushed to 10–20 mesh was dipped into 50 ml of water in a Teflon mini-autoclave beaker within an oven kept at 90 °C for 20 days. The total surface area of the grains was estimated by the following:

$$S = \frac{WS_0}{\rho} \quad (1)$$

where W and ρ are the mass in g and the density in g/cm^3 of sample, and S_0 the specific surface of crushed specimen, respectively. The leach rates of gross and each constituent element were determined from the total weight loss of the specimen and the leachate analysed by inductively coupled argon plasma spectroscopy (ICP).

Table 1
Composition of simulated nuclear wastes

Waste element	Raw material	mass%
Na	$NaNO_3$	64.8
Sr	SrO	2.9
La	La_2O_3	16.1
Mo	MoO_3	7.5
Mn	MnO_2	1.2
Fe	Fe_2O_3	6.6
Te	TeO_2	0.9

2.3. Density, XRD and DTA

The density of the waste forms was measured at room temperature using the Archimedes method with kerosene as the immersion fluid. Powder X-ray diffraction (XRD) analysis of the as-quenched melt was used to verify the amorphous state of the samples. The differential thermal analyses (DTA) were performed in flowing air at a heating rate of 20 °C/min.

2.4. FT-IR and Raman spectra

The FT-IR spectra were measured using the KBr pellet technique in the frequency range 400–4000 cm^{-1} at room temperature. The Raman spectra were measured using a double grating spectrometer with an argon ion laser, scattered radiation being collected at 90° to the incident beam. The spectra were recorded over the 400–1400 cm^{-1} range at room temperature.

3. Results and discussion

3.1. Vitrification of wastes with M–P glass matrix

The composition and density of the M–P glass waste forms prepared in this study are listed in Table 2, where the structure of 45M55P0W (M/P < 1) glass is referred to as the type T, and that of 50M50P0W (M/P = 1) and 55M45P0W (M/P > 1) glass is referred to as the type P. The density increases with increase in simulated HLW content. The glass states were confirmed by the absence of XRD peaks. Only the 55M45P25W glass waste form partially crystallized during cooling. The appearance of the base glass is colorless and transparent. The colors of the glasses, which contain the simulated HLW, are dark brown and turn darker with increasing the simulated HLW content. The borosilicate glasses are limited to no more than 5 mass% actinides. In contrast, M–P glass with up to 55 mol% P_2O_5 can accommodate up to 45 mass% of simulated HLW.

Table 2
Composition and density of glass waste forms prepared in this study

Composition (mol%)	Simulated waste content (mass%)	Waste form	Density (g/cm^3)
$MgO:P_2O_5$ = 45:55	0	45M55P0W	2.45
	25	45M55P25W	2.67
	45	45M55P45W	2.91
$MgO:P_2O_5$ = 50:50	0	50M50P0W	2.25
	25	50M50P25W	2.73
	45	50M50P45W	2.89
$MgO:P_2O_5$ = 55:45	0	55M45P0W	2.51
	25	55M45P25W	2.76
	45	55M45P45W	3.02

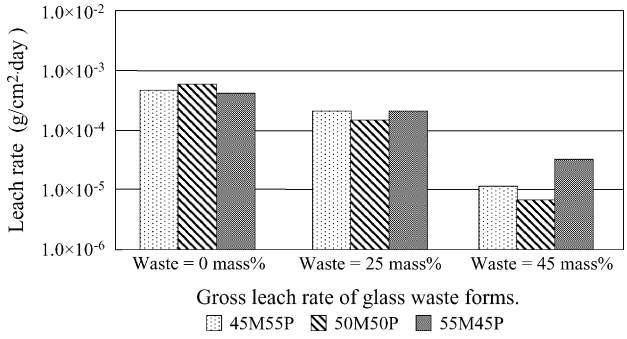

Fig. 1. Gross leach rate of glass waste forms.

3.2. Leach rates of samples in water

The gross leach rates and the leach rates of each constituent element of the sample in water at 90 °C were determined from the total weight loss of the specimen and chemical analysis of leachate solution. The results are summarized in Fig. 1 and Table 3. The chemical durability of the glasses was greatly improved as the addition of simulated HLW. Fig. 1 shows that 50M50P45W has the gross leach rate of the order of 10^{-6} g/cm^2 day, which is fairly low as compared with that of the borosilicate waste glass. Of the elements in most phosphate glasses, Na shows higher leach rate than others, probably because of rather higher solubility of its polyphosphate consisting of chains of phosphate ions. No effect of Na in the M–P glass waste form on its leachability was found. These results can be attributed to the glass structure.

Table 3
Leach rate of each constituent element of 55M45P45W glass waste form

Element	55M45P45W (g/cm^2 day)
Mg	4.79×10^{-7}
P	1.08×10^{-6}
Na	7.35×10^{-7}
Sr	1.00×10^{-9}
La	n.d.
Mo	1.80×10^{-7}
Mn	2.00×10^{-9}
Fe	1.60×10^{-8}
Te	1.00×10^{-9}

3.3. Thermal properties of glass waste form

It is important to obtain information about the thermal stability of the glass waste form, since the crystallization of glass

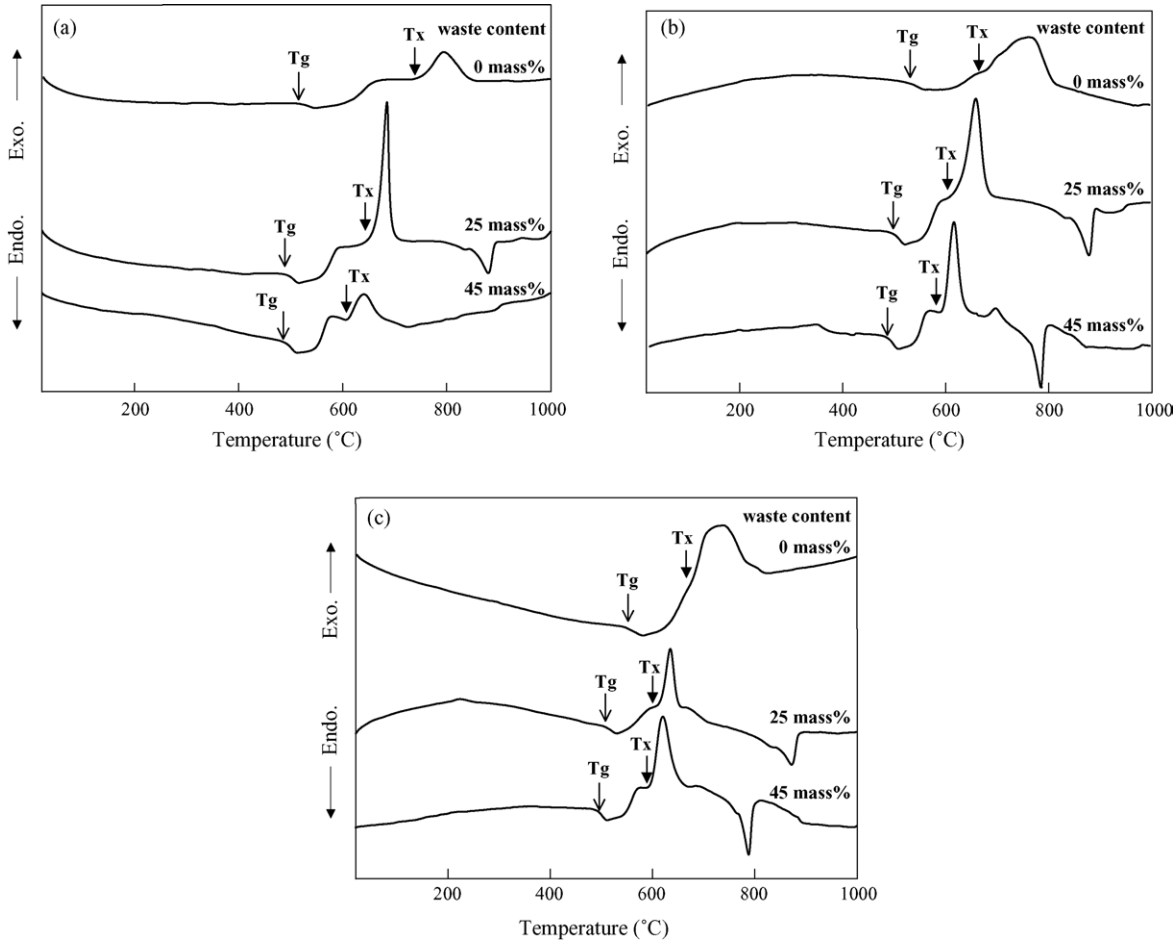

Fig. 2. DTA curves for samples with simulated waste content (0, 25 and 45 mass%). (a) 45M55P, (b) 45M55P, (c) 45M55P.

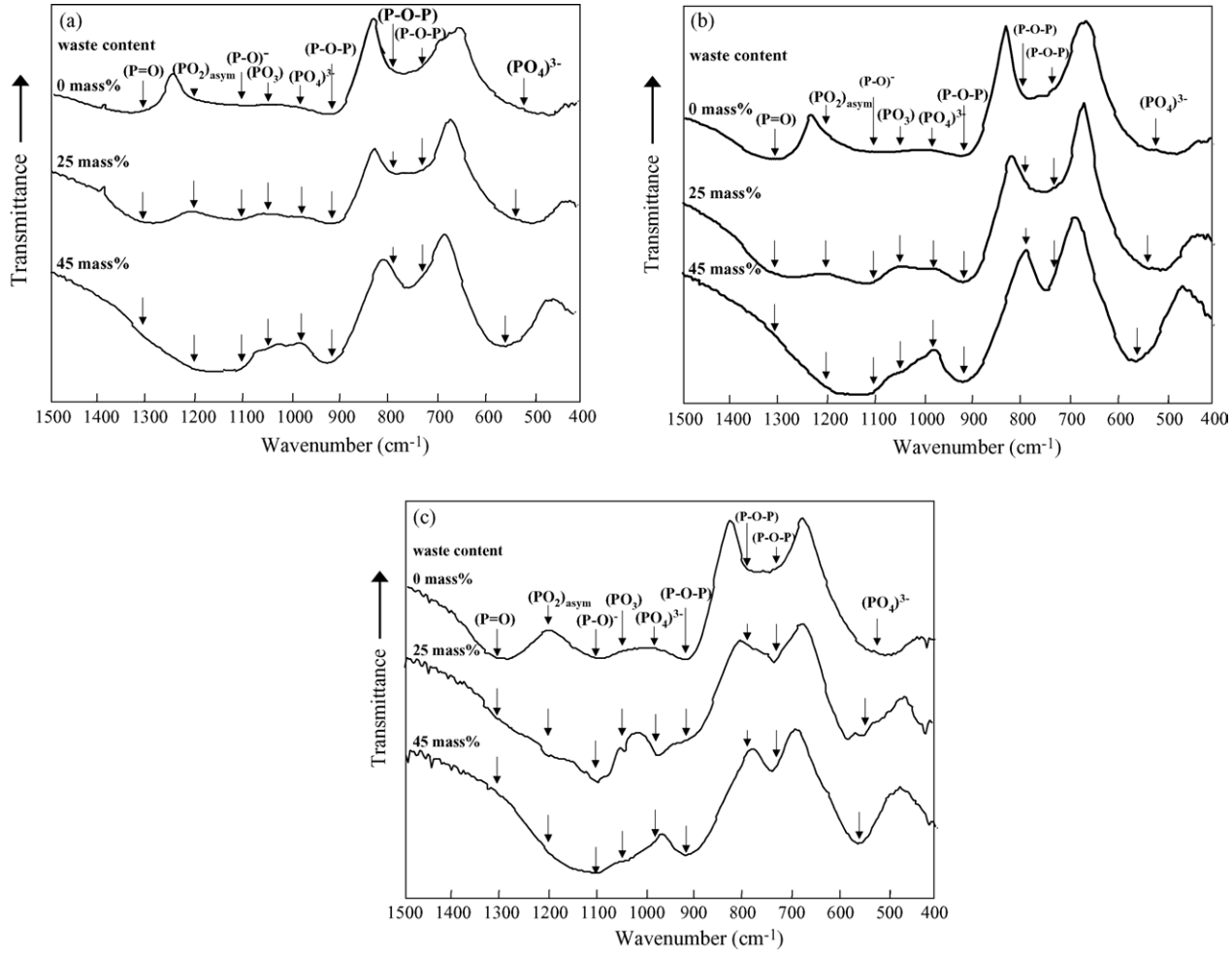

Fig. 3. FT-IR spectra of glass waste forms. (a) 45M55P, (b) 50M50P, (c) 55M45P.

waste can mostly increase the undesirable aqueous corrosion rate of the form, probably due to the formation of somewhat more soluble crystals or the increase in surface area.

Fig. 2 shows the DTA curves of the samples. The starting temperature of the crystallization peaks (Tx) and glass transition temperature (Tg) determined from the DTA curves and the stability of the waste forms (Tx – Tg) are listed in Table 4. The stability of the waste forms with the type P glass matrix does not change with increasing the simulated HLW content.

3.4. FT-IR spectra of glass waste form

The FT-IR spectra of the samples listed in Table 2 are shown in Fig. 3. The strong band near 1300 cm^{-1} is attributed to (P=O) stretching mode. The band obviously becomes smaller indicating a decrease in the double bond character and in the effective force constant of the (P–O) bond as found in ultraphosphates with increasing the simulated HLW content.

The band near 1200 cm^{-1} is assigned to asymmetric stretching modes of the two non-bridging oxygen atoms bonded to phosphorus atoms, $(PO_2)_{asym}$ or Q^2 units, in the phosphate tetrahedra. Their amplitudes obviously increase with increasing waste content. This result indicates that the phosphate linkages are shortened as the simulated HLW incorporate into the glass structure and leading to increase the relative content of the Q^2 units.

The absorption bands near 1100 cm^{-1} have been assigned to $(P–O)^-$ groups and its amplitudes increase with increasing waste content. It is suggested that the absorption bands of (M–O–P) (M = waste element) also locate at near 1100 cm^{-1}, and the relative content of these bonds increase with increasing waste content leading to increased intensity of 1100 cm^{-1} band.

The intensity of the band near 1050 cm^{-1}, which is assigned to (PO_3) end groups (Q^1), tends to decrease with increasing waste content. The absorption bands near 980 and 480–570 cm^{-1} are assigned to the stretching and deformation modes of $(PO_4)^{3-}$ groups (Q^0), respectively. It is shown that the absorption bands of the deformation modes of $(PO_4)^{3-}$ group shift to higher frequencies, and the amplitudes of $(PO_4)^{3-}$ group's absorption bands near 980 cm^{-1} decrease with increasing waste content. The Q^1 and Q^0 groups decrease with increasing waste content. These results indicate

Table 4
The results of DTA measurement of glass waste forms

	Waste forms								
	45M55P			50M50P			55M45P		
	0 W	25 W	45 W	0 W	25 W	45 W	0 W	25 W	45 W
Tg (°C)	519	492	490	553	509	495	541	506	489
Tx (°C)	754	658	609	684	617	596	681	614	598
Tx – Tg	235	166	119	131	108	101	140	108	109

Tg: glass transition temperature, Tx: starting temperature of crystallization.

that the relative content of non-bridging oxygen (P–O^-), which may be replaced by the formation of (M–O–P) bonds, decreases as the incorporation of the simulated HLW.

The absorption bands near 920 and 720–790 cm^{-1} are assigned to the asymmetric and symmetric stretching modes of the (P–O–P) linkages, respectively. The asymmetric stretching band of (P–O–P) near 920 cm^{-1} initially shifts to higher frequencies as the amount of the waste increases. The larger wavenumber of the (P–O–P) band is a result of the smaller (P–O–P) bond angle, which results from shorter phosphate linkages or smaller metal cation size. The phosphate linkages of the glasses with higher waste content are shorter due to the depolymerization of the glass structure.

The formation of asymmetric bridging oxygen (M–O–P) would increase the cross-link density of the glass network, improving the chemical durability of the glasses.

3.5. Raman spectra of glass waste form

The Raman spectra of the samples listed in Table 2 are shown in Fig. 4. The band near 1300 cm^{-1} is assigned to the symmetric stretching mode of terminal oxygen (P=O).

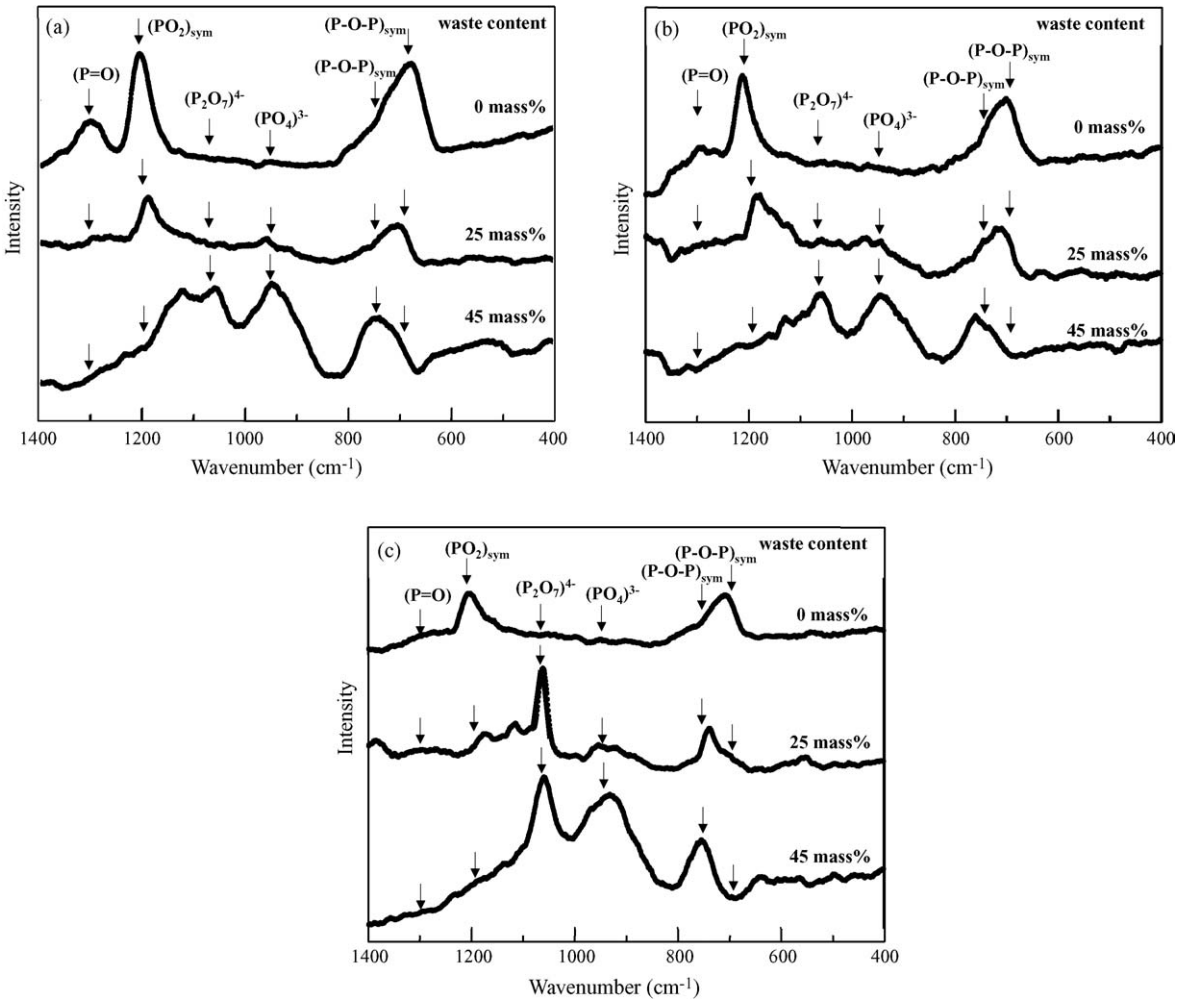

Fig. 4. Raman spectra of glass waste forms. (a) 45M55P, (b) 50M50P, (c) 55M45P.

The bands near 1200 and 700 cm^{-1} are due to the symmetric stretching mode of non-bridging oxygen $(PO_2)_{sym}$ on each tetrahedron and to the symmetric stretching mode of bridging oxygen between two tetrahedral $(P–O–P)_{sym}$, respectively. The bands near 1050 and 760 cm^{-1}, which are characteristic of pyrophosphate groups, are attributed to (P–O) symmetric stretching mode of non-bridging oxygen and (P–O–P) symmetric stretching mode of bridging oxygen, respectively. There are also some traces of orthophosphate groups $(PO_4)^{3-}$ as indicated by the band near 950 cm^{-1}. With increase waste content, the (P=O) stretching mode bands becomes smaller indicating a decrease in the double bond character and in the effective force constant of the (P–O) bond as found in ultraphosphates. Also, with increasing waste content, the bands near 1200 and 700 cm^{-1} have disappeared from the spectrum and the bands near 1050, 760 and 950 cm^{-1} are predominate, that is, the bands characteristic of the pyrophosphate dimer $(P_2O_7)^{4-}$ and orthophosphate monomer $(PO_4)^{3-}$ species increased.

4. Conclusions

M–P glasses are proposed as the potential nuclear waste glasses. The leach rates and structure of M–P glasses loaded with the simulated HLW were examined. The main features of this work are as follows:

(1) Up to 45 mass% loading of the simulated HLW can be incorporated into the base M–P glasses.
(2) The leach rate of the waste glasses decreases with increasing the simulated HLW content. The gross leach rate of the 50M50P45W waste form with the type P glass matrix is of the order of 10^{-6} g/cm^2 day at 90 °C, which is fairly low as compared to that of the borosilicate waste glass.
(3) The stability of the waste forms with the type P glass matrix does not change with increasing the simulated HLW content.
(4) With increasing waste content, the bands characteristic of the pyrophosphate dimer $(P_2O_7)^{4-}$ and orthophosphate monomer $(PO_4)^{3-}$ species increase.
(5) The formation of asymmetric bridging oxygen (M–O–P) increases the cross-link density of the glass network, improving the chemical durability of the glasses.
(6) The type P50M50P glass with low density is most suitable for vitrification of wastes.

References

1. Day, D. E., Wu, Z., Ray, C. S. and Hrma, P., Chemically durable iron phosphate glass waste forms. *J. Non-Cryst. Solids*, 1998, **241**, 1–12.
2. Mesko, M. G. and Day, D. E., Immobilization of spent nuclear fuel in iron phosphate glass. *J. Nucl. Mater.*, 1999, **273**, 27–36.
3. Geel, J., Van Eschrich, H., Heimerl, W. and Grziwa, P., Solidification of high-level liquid wastes to phosphate glass-metal matrix blocks. *IAEA, Vienna*, 1976, 22–26.
4. Grambow, B. and Lutze, W., *Scientific Basis for Neuclear Waste Management, Vol. 2*, ed. CJM, Jr. Plenum Press, New York, 1979, pp. 109–116.
5. Sales, B. C. and Boatner, L. A., Lead-iron phosphate glass: a stable storage medium for high-level nuclear waste. *Science*, 1984, **226**, 45–48.
6. Sales, B. C. and Boatner, L. A., In *Radioactive Waste Forms for the Future*, ed. W. Lutze and R. C. Ewing. North-Holland, Amsterdam, 1988, pp. 193–231.
7. Yanagi, T., Yoshizoe, M. and Nakatsuka, N., Leach rates of lead-iron phosphate glass waste forms. *J. Nucl. Sci. Technol.*, 1988, **25**, 661–666.
8. Yanagi, T., Yoshizoe, M. and Kuramoto, K., Leach rates and thermal properties of lead-iron phosphate glass waste forms. *J. Nucl. Sci. Technol.*, 1989, **26**, 948–954.
9. Reis, S. T., Karabulut, M. and Day, D. E., Structural features and properties of lead-iron-phosphate nuclear waste forms. *J. Nucl. Mater.*, 2002, **304**, 87–95.
10. Shin, P. Y., Properties and FTIR spectra of lead phosphate glasses for nuclear waste immobilization. *Mater. Chem. Phys.*, 2003, **80**, 299–304.
11. Lutze, W., In *Radioactive Waste Forms for the Future*, ed. W. Lutze and R. C. Ewing. North-Holland, Amsterdam, 1988, pp. 1–159.
12. Reis, S. T. and Martinelli, J. R., Cs immobilization by sintered lead iron phosphate glasses. *J. Non-Cryst. Solids*, 1998, **247**, 241–247.
13. Mesko, M. G., Day, D. E. and Bunker, B. C., Immobilization of CsCl and SrF2 in iron phosphate glass. *Waste Manag.*, 2000, **20**, 271–278.
14. Spence, R. D., Gilliam, T. M., Mattus, C. H. and Mattus, A. J., Laboratory stabilization/solidification of surrogate and actual mixed-waste sludge in glass and grout. *Waste Manag.*, 1999, **19**, 453–465.
15. Okura, T., Yamashita, K. and Kanazawa, T., A structural explanation for the phosphate glass anomaly. *Phys. Chem. Glasses*, 1988, **29**, 13–17.
16. Okura, T., Miyachi, T. and Monma, H., Immobilization of simulated high level nuclear wastes with magnesium phosphate glasses. *Mater. Res. Soc. Jpn.*, 2004, **29**(5), 2175–2178.
17. Ishida, M., Yanagi, T. and Terai, R., Leach rates of composite waste forms of monazite-and zirconium phosphate-type. *J. Nucl. Sci. Technol.*, 1987, **24**, 404–408.
18. Strachan, D. M., In *Scientific basis for nuclear waste management*, ed. J. D. Moor. Plenum Press, New York, 1980, pp. 347–348.